宇 宙 科 学 研 究 所 報 告
特集 第30号 1992年2月

New Hard X-ray/Gamma-ray Telescope-Welcome－1－ and Observation of SN 1987 A

By

T. Takahashi[*1], J. Braga[*5], S. Gunji[*1], T. Kamae[*1], S. Miyazaki[*1], H. Murakami[*4], A. Neri[*5], M. Nomachi[*3], Y. Sekimoto[*1], M. Tanaka[*1], T. Tamura[*1] N. Yamaoka[*1] and T. Yamagami[*2]

Abstract: We have developed a new kind of phoswih counters (the well-type phoswich counter) that is capable of detecting very low flux hard X-rays/gamma-rays (60－800 keV) from astronomical object. We flew the first prototype detector system (Welcome-1) from Cachoeira Paulista, Brazil in November 1990. The objective was to detect ^{57}Co (122, 136 keV) and continuum emission from SN1987A. The background spectrum taken at an altitude of 4 g/cm^2 indicates that the 3σ sensitivity reaches ～a few $\times 10^{-6}$/cm^2/s/keV and $\sim 10^{-4}$/cm^2/s by 10^4s observation for the continuum spectrum and line spectrum respectively.

1. Introduction

The precise measurements of hard X-rays and gamma-rays from distant astronomical sources such as supernova remnants and active galactic nuclei are very important in understanding the high energy phenomena in the universe. In these energy range, however, the signal from objects is weak compared with the background. Thus the sensitivity of a celestial

*1 Dept. of Physics, Univ. of Tokyo, Bunkyo-ku, Tokyo 113
*2 Inst. of Space Astro. Science, Sagamihara, Kanagawa 229
*3 Nat. Lab. for High Energy Phys. (KEK), Tsukuba, Ibaraki 305
*4 Dept.of Physics, Rikkyo Univ., Toshima-ku, Tokyo 171
*5 Instituto Nacional De Pesquisas Espaciais, SP, BRASIL

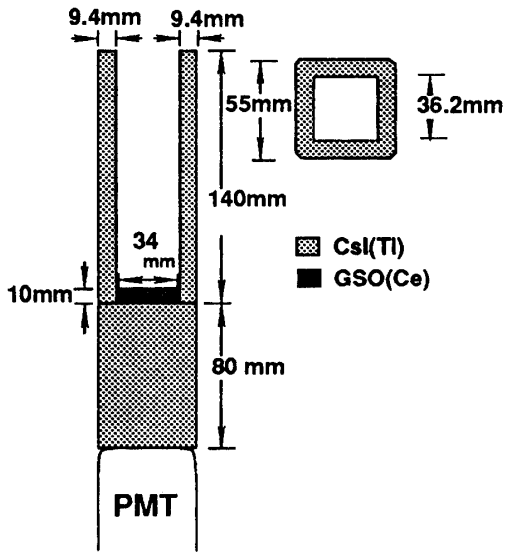

Fig. 1 The schematic drawing of the well-type phoswich counter unit.

hard X-ray and gamma-ray detector has been limited by its siganl to noise ratio.

To reduce the background, we have to shield the detector from various external sources and reduce internal background sources. For energy around a few hundred keV, Compton scattering in the shield becomes appreciable background. The active collimator/shield provides lower background environment than the passive collimator/shield system, because the active system can detect the Compton scattering in the collimator/shield crystal and thereby suppress such events. Traditionally, the active collimator/shield system is realized by the active shield in a phoswich configuration and by additional active or passive collimators.

In order to detect the emission of hard X-rays/gamma-rays at a level of 10^{-6}/cm^2/s/keV, one needs a detector which can realize very low background environment with approprete detector size. A new type phoswich counter (the well-type phoswich counter) presented here fullfills the above requiremens.

2. Well-type Phoswich Counter

In the well-type phoswich counter, a small inorganic scintillator with a fast decay time (the detection part) is glued to the interior bottom surface of a rectangular well-shaped block of another inorganic scintillator with a slower decay time (the shielding part) as shown in Fig. 1. It differs from the conventional phoswich counter in that it has a long protruded collimation part. The well-shaped shielding part acts as an active collimator

as well as an active shield. This configuration not only reduces the background from external sources effectively but also anti-outs most of the internal nuclear activation background.

In the first well-type phoswich counter, GSO(Ce) (Gd_2SiO_5 doped by Ce) is used as the detection part and CsI(Tl) is used as the shielding part. GSO (Ce) is newly developed inorganic scintillator by Hitachi Chemical [*1, 2*]. When GSO (Ce) is used as a detection part in the phoswich counter, its merits are (See Table. 1): (1) the scintillation light decays much faster (60ns) than widely used inorganic scintillators (the decay time of CsI(Tl) is 1μs); (2) the light yield is reasonably high; (3) the attenuation coefficient for gamma-ray is large. For example, the full peak efficiency of 1cm thick GSO (Ce) and NaI (Tl) at 511keV is 30% and 10%, respectively.

The size of the GSO crystal placed in the well is $3.4\times3.4\times1.0cm^3$. The shielding part consists of the collimation part of 0.94cm thick and 14cm long and the bottom shild of $5.5\times5.5\times8.0cm^3$.

In the well-type phoswich counter, the light collection efficiency in the shielding/collimation part becomes important. It requires sufficiently high light-collection efficiency even at the edge of the collimation part such that we can detect a small signal due to Compton scattering of the background gamma-rays. Measurements have shown that the light from the tip of the protrude part is attenuated only by 5−10%, giving a light collection efficiency higer than we expected. Because of the high light collection efficiency, the Compton scattered "background" are suppressed very effectively in the prototype counter.

The energy resolution of GSO scintillator ($3.4\times3.4\times1.0cm^3$) is measured to be 19.4% at 122keV and 8.4% at 511keV gamma-reys. Te light from GSO in the well, however, is attenuated to 50−60% when traversing the shielding part (8 cm of CsI). The energy resolution of 28% at 122keV and

Table 1 Selected High Light-Yield Inorganic Scintillators

	NaI(Tl)	CsI(Tl)	CsI(Na)	GSO(Ge)	BGO
Density (gcm^{-3})	3.67	4.51	4.51	6.71	7.13
Eff. Atomic No.	50	54	59	74	
Index refr.	1.85	1.80	1.84	1.85	2.15
λ_{peak}(nm)	~410	530~580	~420	430	480
Ph. (10^4/MeV)	3.8	5.2	3.9	1.7	0.82
Decay time (ns)	230	~1000	~650	60	300
Att. l. (cm) @511keV	2.94	1.8	1.8	1.48	1.05
Rad. length (cm)	2.59	1.86	1.86	1.4	1.12
Hydroscopic ?	yes	little		none	none

12% at 511keV gamma-rays are achieved in the well-type phoswich configuration.

3. Welcome-1 detector

3.1 Overview

A detector system which utilizes the well-type phoswich counter has been built for balloon-borne experiments. The detector called Welcome-1 (Well type Compound Eye) is designed for the low background observation in the energy range from 60keV to 800−1000keV.

The detector consists of 64 GSO(Ce)/CsI(Tl) well-type phoswich count-

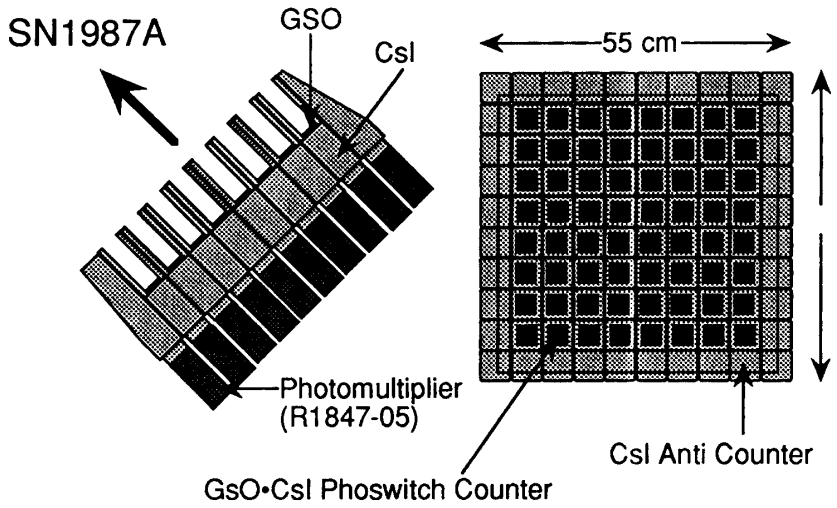

Fig. 2 The first detector system based on the well-type phoswich counters. The whole detector system consisting of 8×8 well-type phoswich counters and 36 dedicated shieding counters.

Table 2 Characteristics of the Welcome-1 telescope

Energy range	60keV−800keV
Type	64 well-type phoswich counters detection part: GSO 3.4×3.4×1.0cm^3 shielding/collimation part: CsI(Tl) 8×8 matrix configuration 36 CsI anti counters
Total area	740cm^2
Full peak efficiency	100% at <200keV 30% at 511keV
Energy resolution	28% at 122keV 12% at 511keV
Aperture	±7.4°
Time resolution	32 μsec
Weight (includes the gondola)	680kg

ers assembled in the "compound-eye" configuration as shown in Fig. 2. Each counter is viewed by a single 2-inch photomultiplier individually. The signal from the photomultiplier is fed to the specially designed electronics described below. In the compound eye configuration, each element is surrounded by eight neighboring elements which serve as additional active shields for the particular element. Thus the detector system can easily be expanded while keeping the effective anti-counting rate per element reasonably low.

Table 2 summarizes the basic characteristics of the Welcome-1 detector. The effective area of the detection of Welcome-1 is 740cm^2 for 122keV line and 222cm^2 for 511keV line. The field of view (FOV) of the detector is determined by the detection efficiency of the protruded part of the well. For 122keV lines, the measured value of the FOV is $\pm$7.4 degree and is consistent with the geometrical value. For 511keV lines, it becomes $\pm$9 degree. 36 CsI(Tl) crystal surrounds the phoswich counters as an additional shield for the outermost counters.

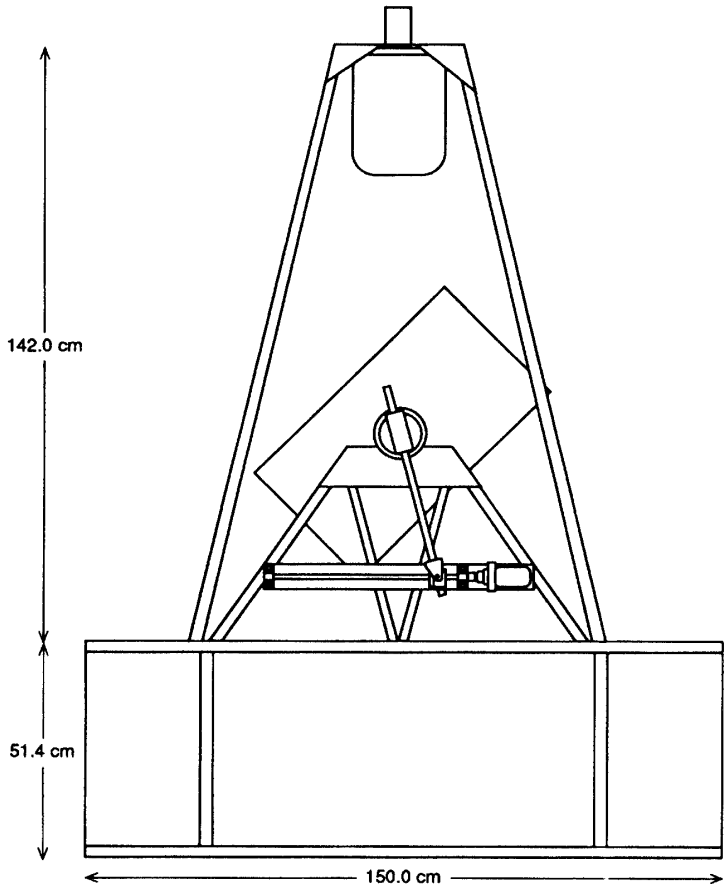

Fig. 3 The schematic drawing of the Welcome-1 detector and the gondola.

The schematic view of the Welcome-1 telescope and its gondola are shown in Fig. 3. There are 64 well-type phoswich counters 36 shield crystals stored in the Al-honeycomb box and the box is attached to a gondola by two bearings which allows changes in the elevation angle of the telescope, The elevation angle is controlled by a ball screw drive located on the gondola. Electronics system, telecommunication equipments and batteries are mounted inside the gondola.

On the top of the gondola, a torque motor is attached. The whole instrument is suspended by the straps through the motor axis. Azimuth pointing and rotation are achived "Yorimodoshi" method. A magnetometer on the gondola and the troque moter forms the stabilization system.

3.2 Electronics System

The electronic system of the telescope for a balloon-borne experiment is the most difficult part because of its operating environment. We must ensure the proper operation even at an altitude of 40km where the atomos-

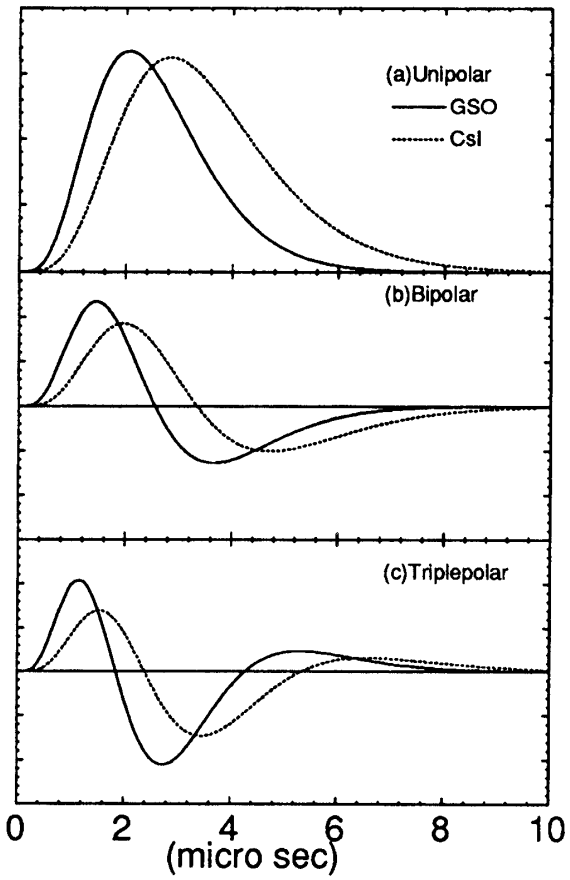

Fig. 4 The wavefrom of (a) unipolar, (b) bipolar, and (c) tripleiar pulses by 500ns time constant (RC) inthe shaping amplifier for GSO signal (solid line) and CsI signal (dotted line).

pheric pressure is 4mb and thus the operating temperature of the circuit reaches 60－70 degree. The electronic system for the Welcome-1 is specially designed to process data from many channels under nominal constrants for space experiments: low power consumption, high reliability and compactness[3].

3.2.1 Analog Electronics

Because of the large volume of the shield crystal, the shield (clean hits on GSO(Ce)) to the noise (hits on CsI(Tl) including Compton scattered in CaI(Tl)) ratio is very low. By properly designing an electronic circuit, one can discrimimate against a small admixture of the faster scintillation light. This circuit, pulse shape discriminator (PSD), is thus critical for the successful operation of the phoswich counter. The circuit must be simple and consume as little power as possible, because we have to operate a large number of channels within limited power consumption.

In order to satisfy these conditions, a new PSD circuit was developed[3]. In the present system, signal from the photomultiplier is first fed to charge sensitive preamplifier having the 16μs time constant and then sent to the PSD. The PSD is composed of the shaping amplifier and logic elements.

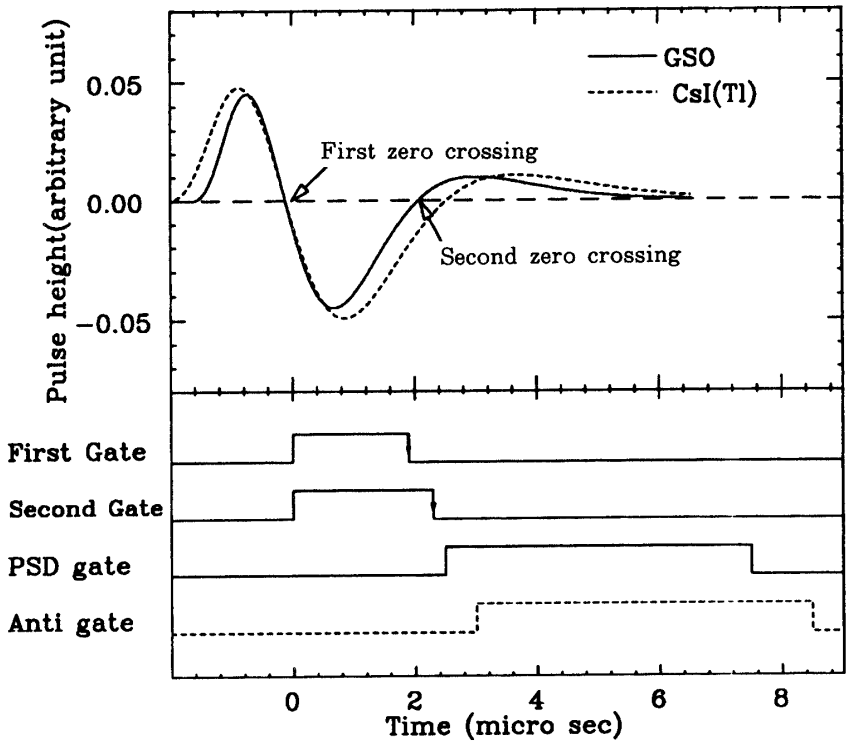

Fig. 5 Principle of the pulse shape discriminator. The PSD pulse is issued only if the second zero crossing point falls inthe first gate and the second gate.

In the shaping amplifier, the signal is differentiated and integrated to form the unipolar, double-polar and triple-polar pulses (See Fig. 4). The time interval between the first and second zero crossing point in the triple polar pulse is sensed by means of two time pick-off circuits.

Using the time constant of $\tau_{RC}=0.5\mu s$ for the shaping amplifier, the difference in the time intervals for GSO(Ce) and CsI(Tl) signals is around 400ns. The lower level discriminator in the first time pick-off circuit defines the minimum energy level accepted. In the input signal exceeds a discriminator level, two logic gates are generated at the first zero crossing timing. If the second zero crossing point falls in between the gates, the PSD circuit issues a "GSO event" pulse (PSD gate) (Fig. 5) at the second zero crossing timing. If the second zero crossing points does not fall in between gates, the "CsI(Tl) event" gate is issued.

To monitor the operation of the PSD, we measured the time interval between the two zero-crossings by TDC. Fig. 6 shows the 2-dim distribution for the TDC counts and the ADC counts produced by calibration sources

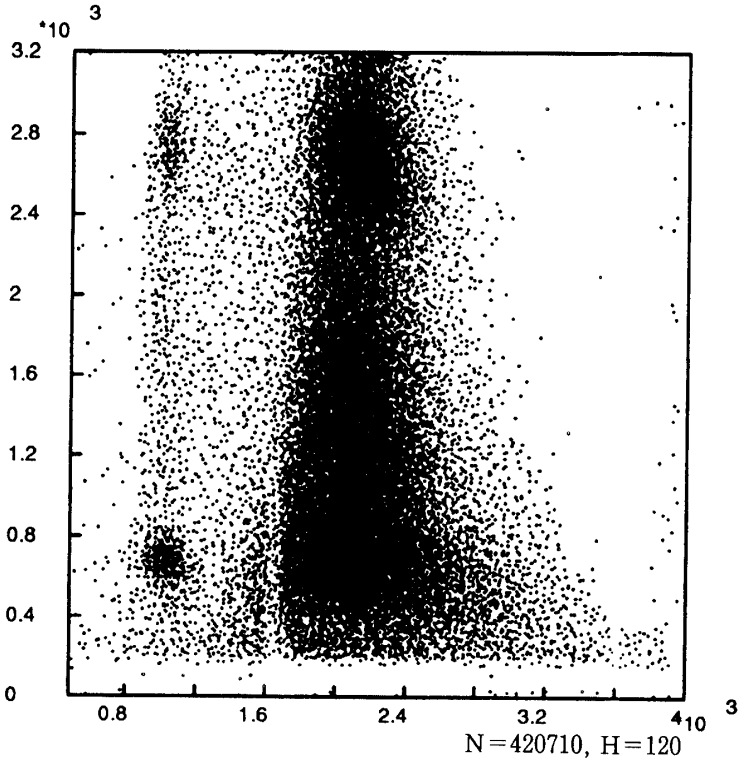

Fig. 6 2-dim distribution of ADC's and TDC's obtained by Welcome-1 when it is irradiated by ^{57}Co and ^{22}Na. The band on the left corresponds to GSO (Ce) events and the band on the roght corresponds to CsI(Tl) events.

(122keV line from ^{57}Co and 511keV line from ^{22}Na). In the plot, the band on the left corresponds to GSO(Ce) events and the band on the right is due to the events in which hard X-rays/gamma-rays deposited some or all energy in the CsI(Tl) shield crystal.

Fig. 7 is the projection of Fig. 5 onto X-axis and shows the distribution of the TDC counts. The PSD performance is demonstrated in Fig. 8 where the energy spectra with and without PSD gate are shown. By applying the PSD gate, the background due to Compton scattering events and events in which the hard X-rays/gamma-ray deposited its energy in the shield are suppressed. In the figure, two peaks are clealy seen.

When the number of photo-electrons becomes low ($n_e \leq 50$ or $E \leq 50$keV),

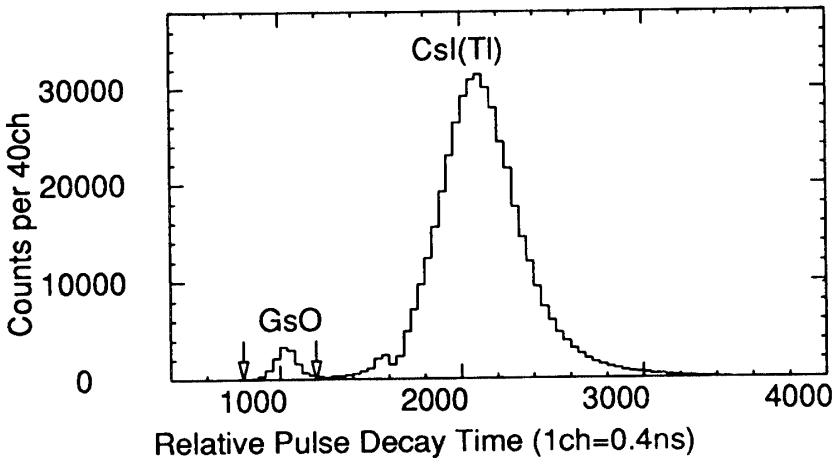

Fig. 7 Distribution of TDC counts obtained by external sources. The peak on the left corresponds to GSO(Ce) events. The position of the first gate and the second gate to select GOS(Ce) are also shown.

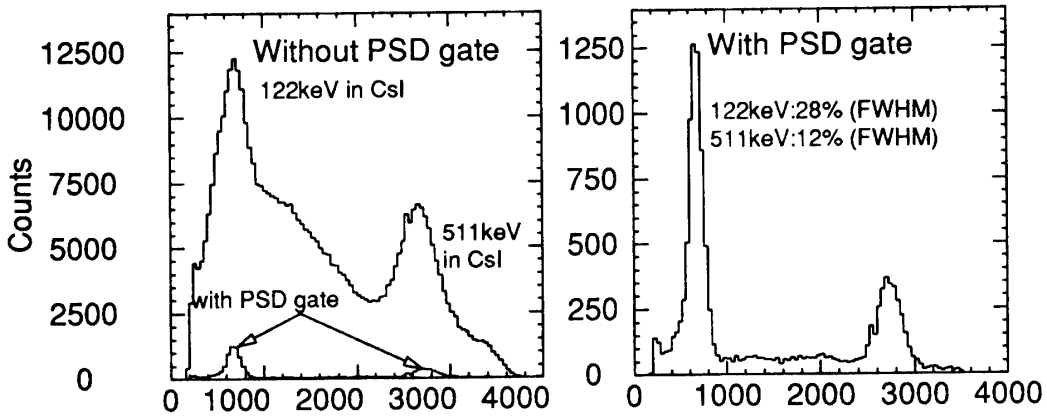

Fig. 8 Energy spectra for ^{57}Co and ^{22}Na: (a) When the PSD gata is not required (the upper curve) and when it is required (lower curve); (b) When the PSD is required (the enlargement of the lower curve in (a)).

the pulse shape of CsI(Tl) pulses fluctuates. If the pulse narrows significantly, they passes through the PSD filter. This seems to set the minimum detectable energy limit of the well-type phoswich counter.

By the new method, we can significantly reduce the effect of the time slewing in the low energy region with a small number of components in the circuit. The PSD is composed of four hybrid IC's, three for the shaping amplifier (150mW/channel/IC) and one for the timing logic (200mW/channel). Sixteen PSD's and additional circuits for monitoring are arranged in two double-width NIM (Nuclear Instrumentation Module) modules

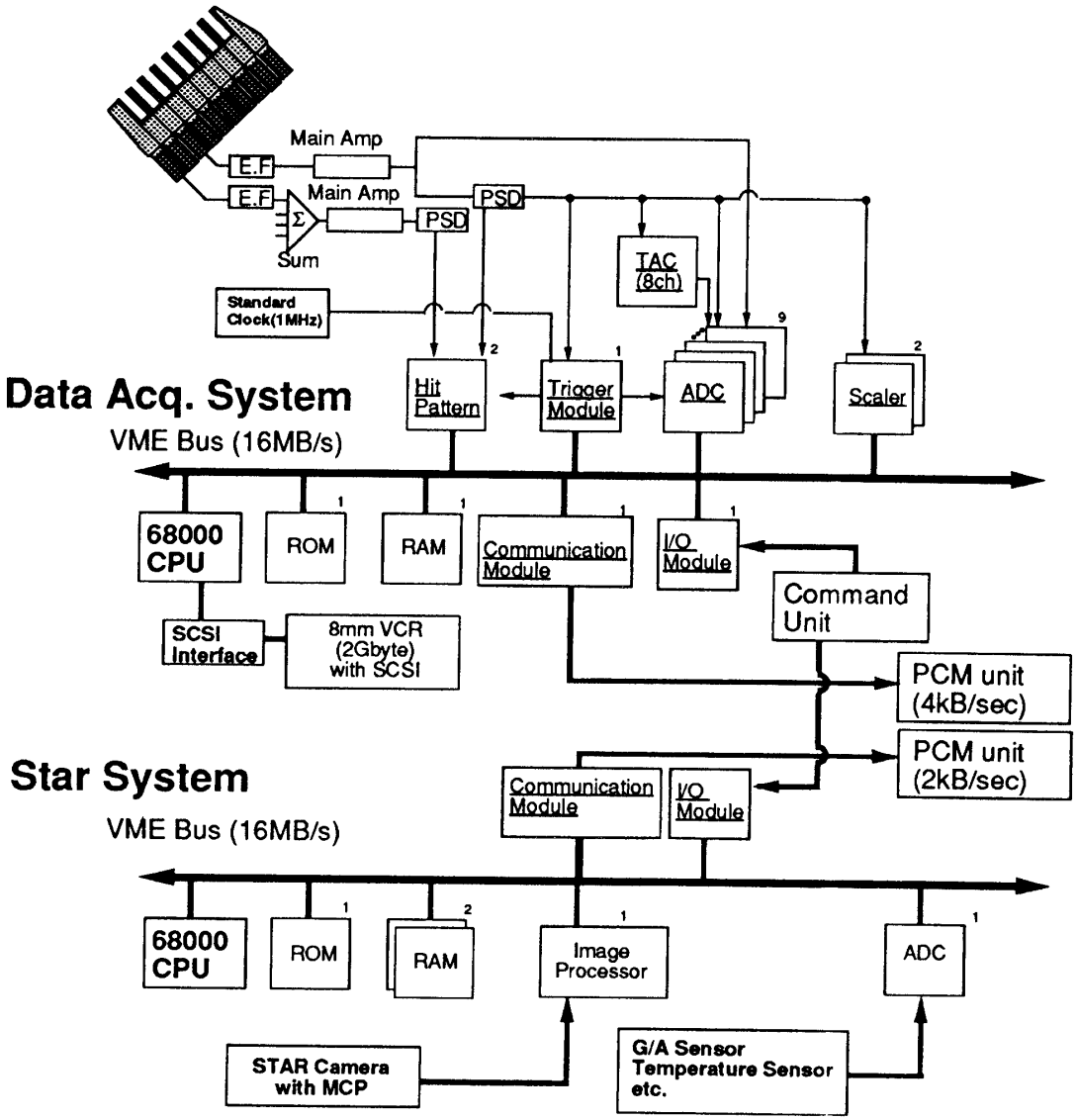

Fig. 9 Schematic drawing of the online system. Upper part of the figure shows the date acquisition subsystem and the lower part of the Fig. shows the star camera subsystem.

(one is for the shaping amplifier and the other is for the timing logic).

3.2.2 Online System

The online system consists of two sub-systems, one is to acquire data from the detector and the other from the star camera. The block diagram of the online system is shown in Fig. 9. Each sub-system is controlled by its own 32 bit microprocessor through VME (Versa Module Eurpoe) bus. The VME standard is a widely used standard for real-time operation in industry and many kinds of modules are commercially available. It supports 32 bit access for both addressing and data trabsfer and facilitates design of a high speed online system.

Data Acquisition Sub-system

In Welcome-1, each element is arranged electronically so that each element acts as an active shield to the neighboring ones. There are 64 PSD signals and 36 antisignals to be processed in the system. Analog output from the shaping amplifier in the PSD is split into two paths: one goes to the logic and the other to ADC. The outputs of four neighboring PSD's are ORed for triggering, forming 16 trigger lines in total. The signals from active anti crystals are summed in analog sum units and sent to the discriminators. Because of the limitation of the space and the electric power, only eight PSD channels are monitored by TDC in flight.

When a trigger signal is generated from one counter, the ADC's in the particular group of four, the hit-pattern of the lower discriminator, and the hit-pattern of the upper discriminator are recorded by the online system together with the time of the event. The hit pattern of neighboring counters is used to reduce background by rejecting events that have been scattered in the neighboring counters. The fact we read out only the nearest neighbors serves to reduce the overall dead time as well as the failure rate of the detector system.

The time of the event is counted to 32 μs accuracy by precision quartz clock with the frequency stability of $\Delta f/f=10^{-9}$/month. This high stability is needed for the study of millisecond pulsars.

The microprocessor is MC 68000 CMOS CPU operated at 10 MHz. The CPU is operated on the software stored in the PROM. Controlling and processing of data is done by a set of interrelated processes and interrupt routines controlled by the real time operating system. The 512kB CMOS RAM provides data buffer in which data is reformatted for the transmission amd recording. Additional microprocessor tasks include collection of status and housekeeping data. Each PSD gate is counted by a 16 bit scaler and the monitor process reads the date every 5 s. The operating modes and

paramenters in the system are changed by ground commands. The Data I/O module receives ground commands and issues interrupt signals to the microprocessor.

The data size per trigger is 24 bytes and the size of monitor data is 312 bytes. The maximum data acquisition rate of this system is 48kB/s which corresponds to the trigger rate of 2kHz. At the expected trigger rate of 150Hz, all data will be transmitted to the ground via telemetry (max 4kB/s).

Star Camera Sub-system

In the star-camera sub-system, a MCP (micro channel plate) coupled to a CCD camera images the sky. Its field of view is 9.1×6.3 degrees and identifies stars of magnitude~8.1. The star image on the CCD camera (512×512 pixels) is digitized by the image processing board on the VME bus. The microprocessor selects the bright points and then transmits brightness and position of each points to the ground through the telemetry (max 2kB/s). On the ground station the star image is reconstructed every 2 seconds by using a workstation.

On Board Data Recording

The data taken by the data acquisition sub-system is recorded on a EXABYTE 8mm VCR via SCSI (Small Computer System Interface) bus. This VCR holds upto 2GB and provides error correction rate less than 10^{-13} bits. In our data acquisition system, a continuous data storage rate of 82kB/s can be achieved.

4. Balloon-borne experiments

4.1 Gamma-rays expected from SN 1987A

SN1987A has given us a golden opportunity to study the supernovae explosion, the nucleosynthesis, and the young neutron star. Observational facts on the light curve, the hydrogen and helium lines in the optical spectrum, the X-rays, the Gamma-rays, etc. now allow us to test theoretical models about the SN1987A remnant, the nuclear composition, density and velocity profile of SN1987A.

Observation of monoenergetic gamma-ray emission gives us direct information on the nucleosynthetic process occurring in the supernova. Two prominent lines, 847keV and 1238keV in the decay of ^{56}Co, have been observed by satellite and balloon experiments. The observed fluxes in about 180 days after the explosion were about $\sim 1 \times 10^{-3}$ photons/cm^2/s for 847 keV line and 6×10^{-4} photons/cm^2/s for 1238keV.

The exponential decay of the light curve is explained well by the hypothesis that gamma-rays from ^{56}Co heat up the outer layes of the remnant.

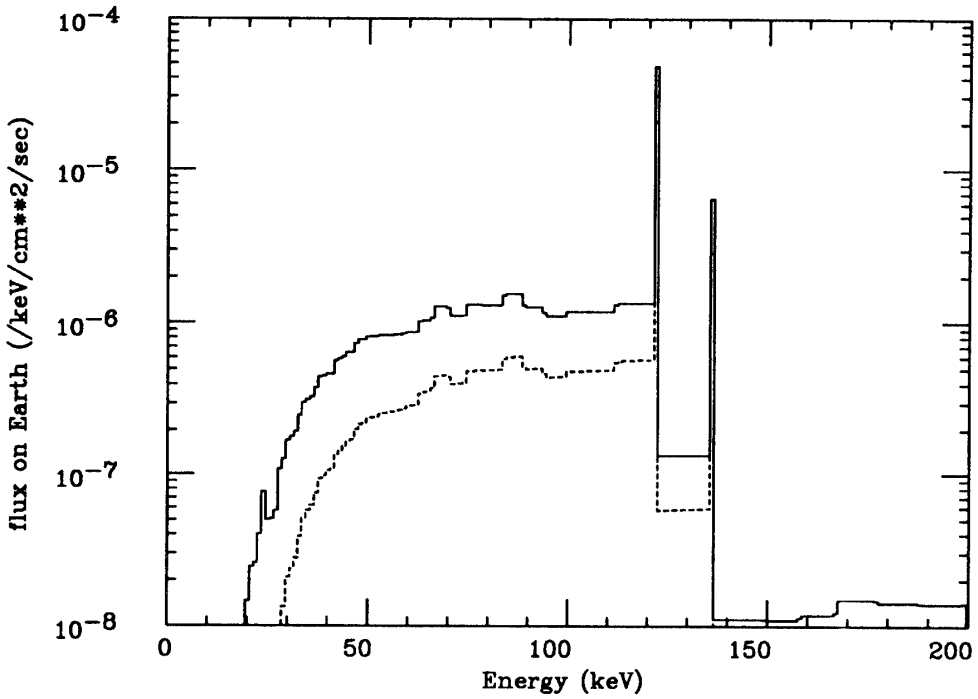

Fig. 10 Expected energy spectrum from the decay of ^{57}Co at 1,400 days after explosion. Solid line shows the spectrum expected at the earth and dashed line shows the spectrum after the attebnuation by 6g air is taken into account.

Compton degradation of these gamma-rays consistently accounts for early emergence and light curve of hard X-rays (10keV−30keV) observed by Ginga.

On the other hand, the slow down of the decline rate in the optical light curve was reported since 900 days after explosion. Two possible energy sources that may account for the slow down are the radioactive decay of ^{57}Co and the emission from the central pulsar[*4*].

According to the calculation by Kumagai *et al.* [*4*], the intensity of emission line of ^{57}Co reaches broad peak some time between 600 days and 1400 days after explosion. The expected X-ray spectrum at 1400 days after explosion is shown in Fig. 10. In the figure, they assumed that the energy is supplied mainly from the radio active decay of ^{57}Co and the ratio $<^{57}\mathrm{Co}/^{56}\mathrm{Co}>$ is equal to 1.7 of the ratio $<^{57}\mathrm{Fe}/^{56}\mathrm{Fe}>$ at the Earth. Note that the ratio higher than 8 is needed to explain the slow down by the ^{57}Co alone. Also shown in the figure is the spectrum in which the attenuation by 6g/cm^2 of the air (namely at an altitude of 4mb) in included.

If the slown down of the decline rate in the light curve is explained by the central pulsar, X-ray luminosity of $10^{37}-10^{38}$erg/s is needed in addition to the cobalt dacay. Fig. 11 shows the light curves of the X-rays the

90－140keV 140－300keV X-rays from the pulsar predicted by the model. In the model, the original pulsar radiation is assumed to have a Crab-like power law spectrum and have the luminosity of the 1×10^{38} erg／s. The light curve of the sum of the flux from the decay of cobalt and the flux by the pulsar is also shown in the figure for 90－140keV energy range.

4.2 Observation of SN 1987A

The Welcome-1 was flown onboard a balloon (2.5×10^5m^3) from the INPE balloon base in Cachoeira Paulista (Brazil) on 29 November 1990 corresponding to 1375 days after explosion of the supernova. The base is located at 45 00 34W and 22 39 44S. The scientific objective of the flight was to detect 122keV and 136keV lines from ^{57}Co and continuum emission from SN 1987A discussed above.

The payload was successfully launched and reached a ceiling altitude of 4g／cm^2. The experiment performed well throughout the flight of 10 hours. Fig. 12 shows the ascent curve of the altitude and the counting rate of the CsI (Tl) anti counter in the house keeping data. The rate reached maximum at～20km (Pfotzer Maximum) and then decreased to the same level as that of the ground level. The typical counting rate of one outermost CsI (Tl) anti

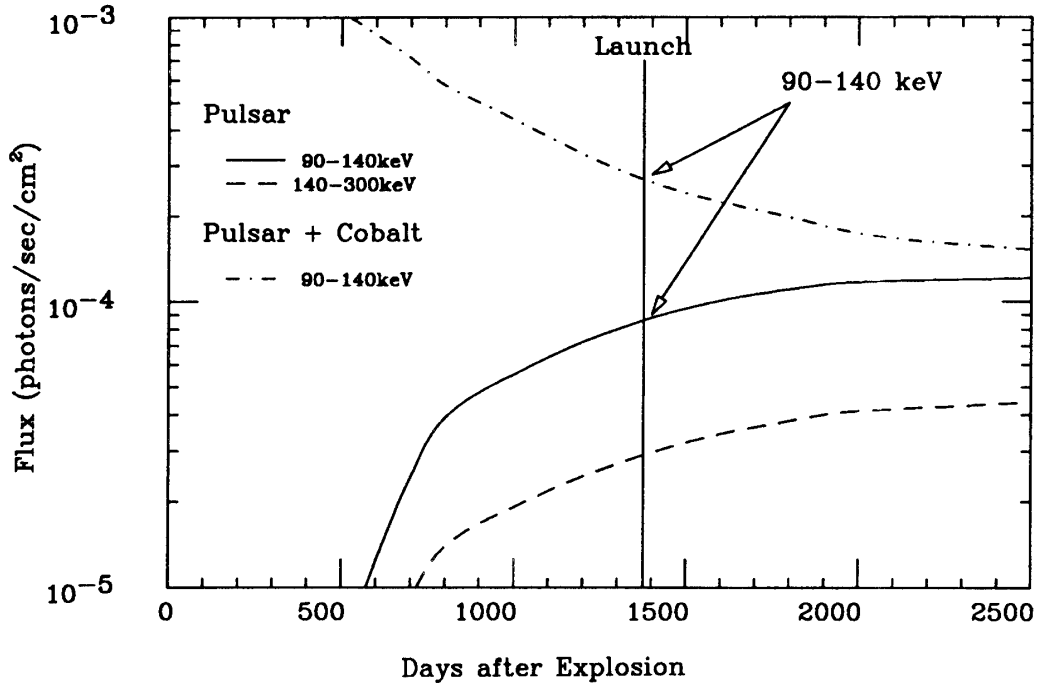

Fig. 11 The light curve obtained from the model calculation. The solid line and the dashed line show the contribution from the crab-like pulsar of $L_x=10^{38}$ erg／s for 90－140 and 140－300keV energy interval, respectively. The dashed-dot line shows the sum of the flux of the decay of ^{57}Co, ^{56}Co and the emission by the pulsar.

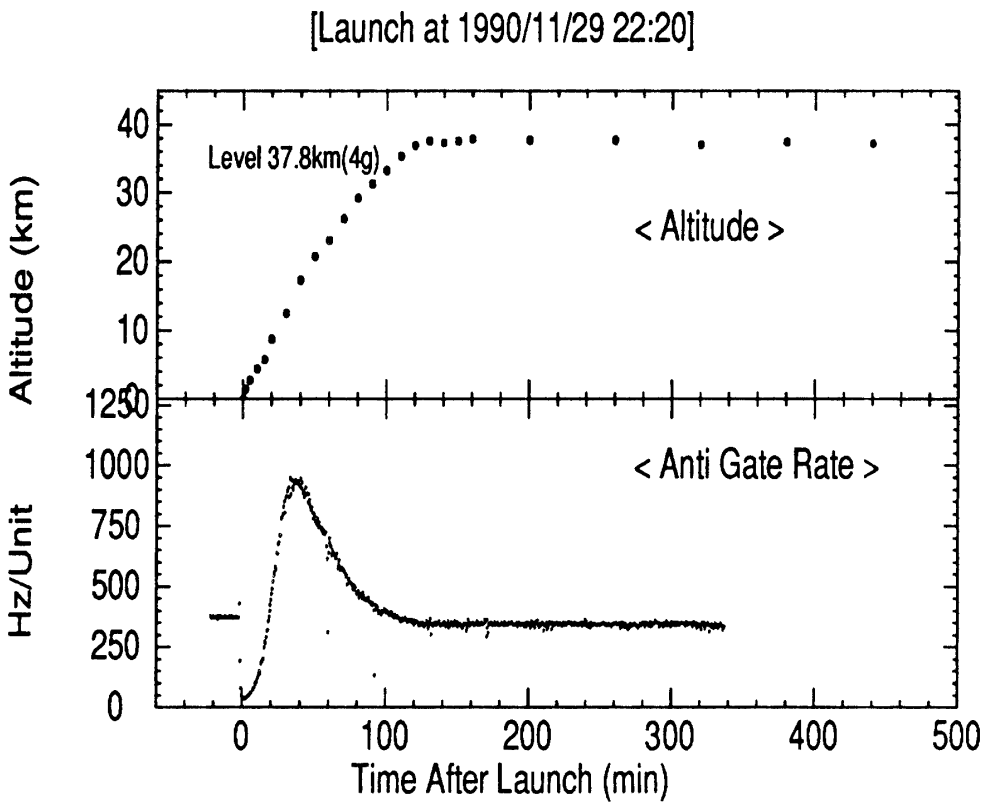

Fig. 12 Ascent curves during the flight of November 29, 1990 : the altitude of the payload (upper figure) and thecounting rate of the outer anti shield made of CsI (Tl) crystals (lower figure).

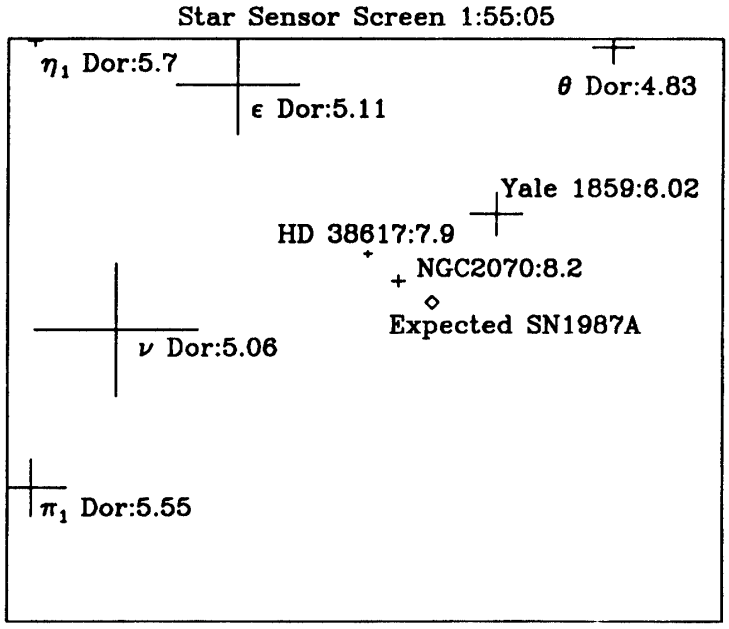

Fug. 13 Reconstructed star image taken by the star camera. The field of view of the image is 6.0°×9.4°.

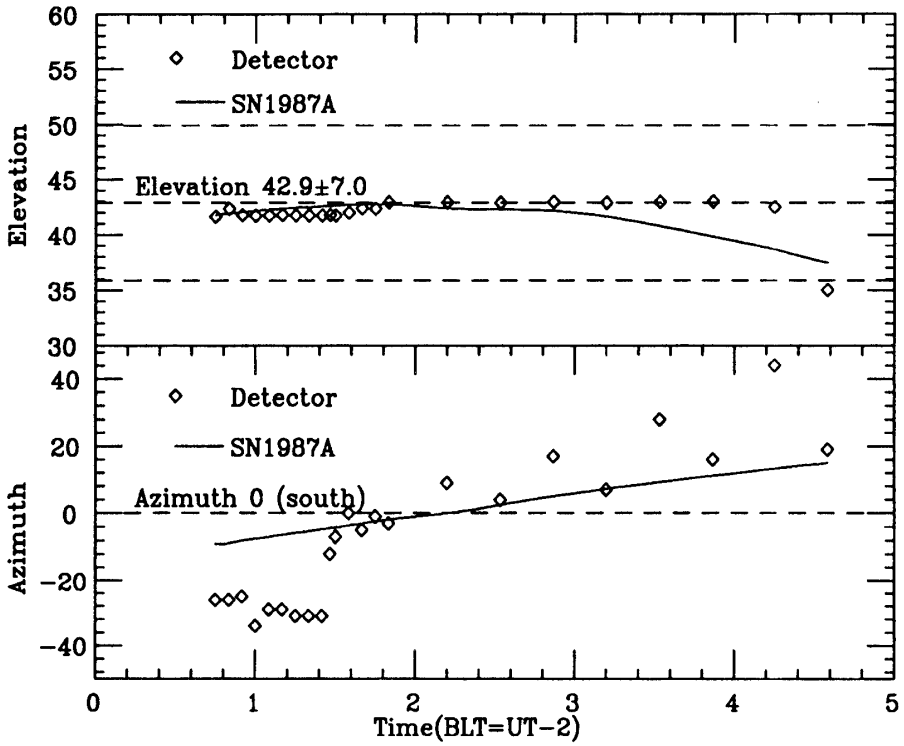

Fig. 14 Elevation and azimuthal angle of the detector during the observation.

counter ($\sim 5.5 \times 5.5 \times 22 cm^3$) was 400Hz at the ceiling.

During the flight, we repeated the on-source observation of SN1987A and the off source background observation every 40 min (20+20 min). The direction of the detector was monitored by the star camera. The reconstructed star image near SN1987A region is shown in Fig. 13. From the star image the direction of the detector was determined within ± 0.02 degree. Fig. 14 shows the elevation and the azimuthal angle the Welcome-1 detector was pointing during the flight. In total, the detected pointed to SN1987A region for 5436s and to Background region for 5367s at the same elevation angle of 42.9 degree.

4.3 Background Spectrum at the Ceiling

Fig. 15 shows the background spectrum obtained at an altitude of $4 g/cm^2$ (37.8km). The spectrum was obtained from one well-type phoswich counter located near the center of the detector. As demonstrated in the figure, the low background environment was realized by the well-type phoswich counter. Using the hit information of the surrounding crystals, background events due to Compton scattering and/or 511keV annihilation lines in the material are clearly suppressed. Background levels at 122keV and 511keV are $1 \times 10^{-4}/cm^2/s/keV$ and $4 \times 10^{-5}/cm^2/s/keV$, respectively.

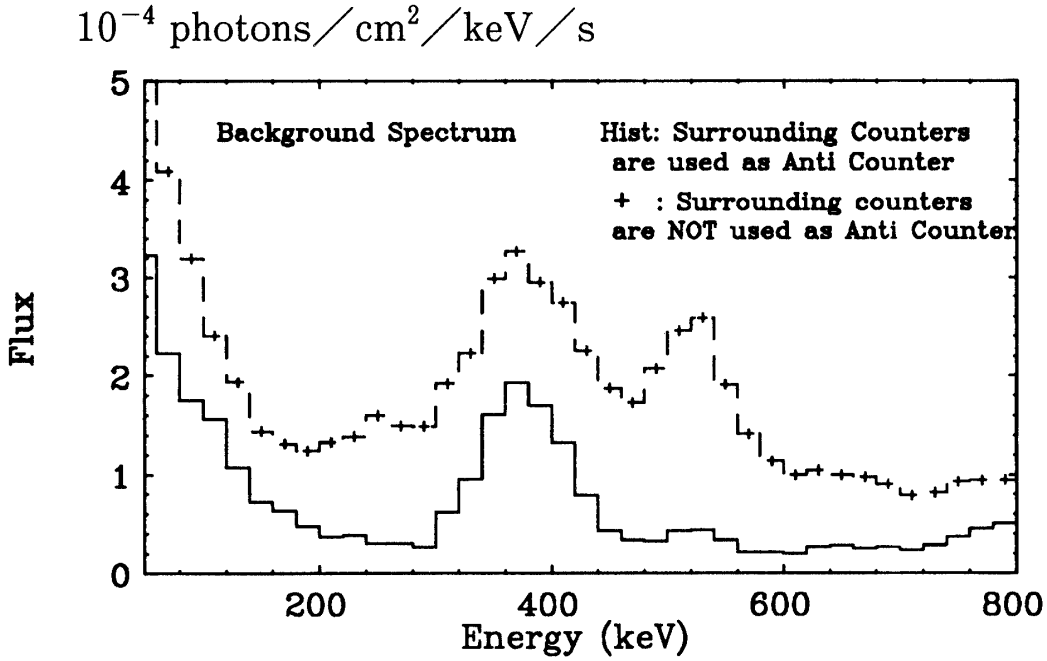

Fig. 15 Back ground spectrum obtained from one unit located near the center of the detector. The altitude is 4g/cm^2 and the effective observation time is 12,300s. The solid and dashed line show the the spectrum taken with and without the background reduction by the surrounding counters, respectively.

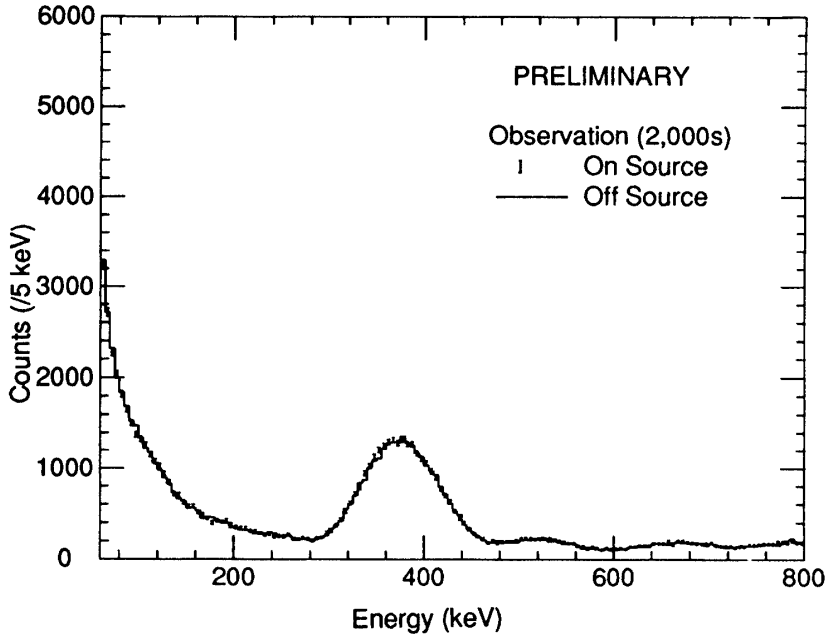

Fig. 16 The on-source and off-source spectrum obtained during the pointing operation to SN1987A. Actual observation time after we corrected the dead time is about 3.350s for each of on-source and off-source observations.

In the figure, a broad peak at 368keV is clearly visible. It is due to ^{152}Gd (natural abundance=0.2%, 2.14MeV α decay, half-life 1.1×10^{14}y) and ^{147}Sm (abundance=15.1%, 2.23MeV α decay, half-life 1.06×10^{11}y). Bumps over 600keV in the spectrum are due to the radioactive contamination from the Thorium and the Uranium series in the GSO crystal. Note that ^{152}Gd is unremovable, but others can be reduced by using higher purity materials.

The peak position of ^{152}Gd can be used to calibrate the channel by channel gain variation and the drift of the gain with time (mostly due to temperature variation: -0.5%/degree for the GSO scintillator). Furthermore, because of its very long life time, the area of the peak is used to calculate the net live time of the detector system.

4.4 Data Analysis

In order to derive the energy spectrum from SN1987A, we must subtract the background spectrum from the on-source spectrum. For this, the gain calibration is crucial. Since the shape of the background spectrum follows a power-law (photon index $\sim$1.7) and the systematic variation of the gain easily introduce a dip or wiggle in the low energy region of the subtracted spectrum. Gain varies with time for several reasons; variations in high voltage, the light yield of the scintillator for a fixed energy deposit, the gain of amplifiers, etc. Using the ^{152}Gd peak, we can correct data for those variations precisely. After the gain was calibrated, background events were rejected using anti-hit pattern.

In the analysis of the data, fits were performed to the ^{152}Gd peak obtained in the 30 min interval for each channel varying the starting point in 5 min step. The gain factors were calculated from the variation of the peak position of ^{152}Gd with time and were applied to each counter. After the correction, the gain was calibrated to an accuracy of $\pm0.15\%$ (RMS) from one channel to another and $\pm0.21\%$ (RMS) for the drift with time.

In Fig. 16, the energy spectrum is shown for both the on-source observation and the background observation. In the figure, the net live time was calculated using the area of the ^{152}Gd peak. Before going to the next step, however, we need to study following possible systematics:

1. Validity of the gain correction
2. Azimuthal dependence of background spectrum
3. Scintillator's non linearity
4. Live time estimation
5. Correction of angular acceptance of the detector

The analysis is progressing steadily and the final conclusion will appear soon.

5. Results

The detector performance, the sensitivity curve of the Welcome-1 calculated form the obtained background spectrum is shown in Fig. 17. The curve represents the three standard deviation sensitivity tat can be achieved in an observation of 10^4s (no attenuation by atmosphere). In Welcome-1, a sensitivity of~a few$\times 10^{-6}$/cm^2/s/keV and ~10^{-4}/cm^2/s by 10^4s observation can be attained for the continuum spectrum and line spectrum respectively.

The sensitivity for ^{57}Co line from SN1987A is calculated from the background spectrum and the net observation time afrer we corrected the live time of the detector system. Currently, the dead time amounts to about 35% which is introduced in the process of rejecting fack events caused by

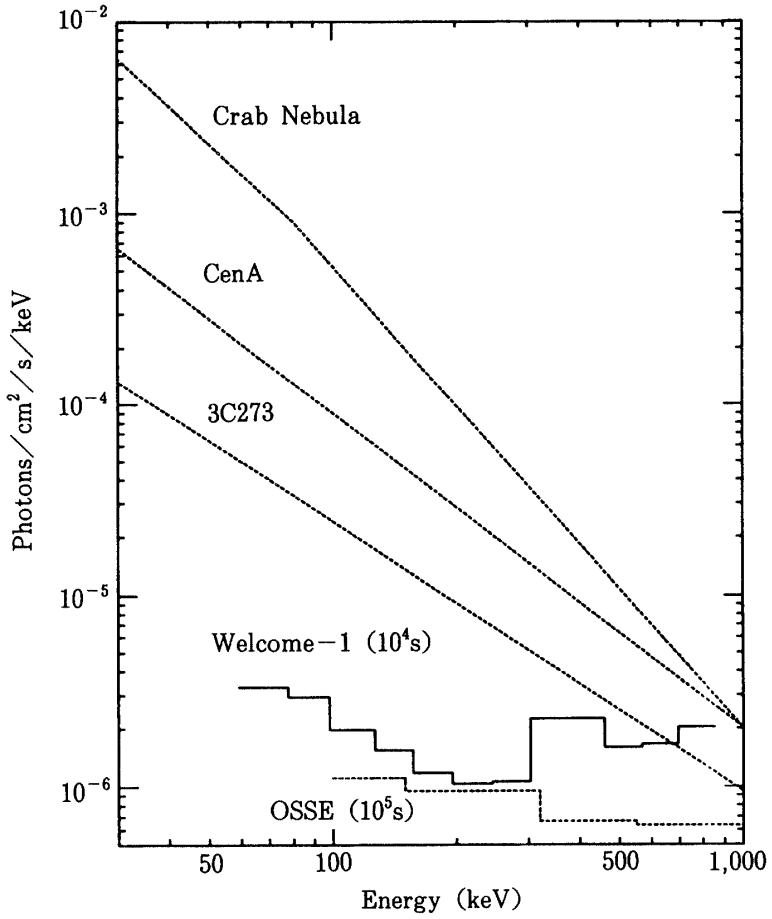

Fig. 17 3σ sensitivity of Welcome-1 for 10,000s (the solid line) and OSSE for 100,000s (the dotted line) [5] for continuum spectrum. X/Gamma-rays are assumed not to be attenuated by the atmosphere. Note that the observation time for Welcom-1 is 10 times shorter and the binning for Welcome-1 is finer than these for OSSE.

energetic charged particles. In spite of the short observation time (~3,350s), the one sigma sensitivity of this observation is $\sim 1.9 \times 10^{-4}$ photoms/cm^2/s in the energy range between 90keV and 140keV. From data obtained in the energy region of 140keV −300keV, the sensitivity also reaches $\sim 1.9 \times 10^{-4}$ photons/cm^2/s.

According to the model calculation [*4*], integrated counts from 90 keV to 140 keV is calculated to be $\sim 1.0 \times 10^{-4}$ photons/cm^2/s for the ratio$<^{57}$Co/^{56}Co$>$ is equal to 1.7 of the ratio$<^{57}$Fe/^{56}Fe$>$ at the Earth. Thus if the ratio is higher than 5.0, the gamma-rays from ^{57}Co decay is detectable in our observation with 90% confidence level. For 140−300 keV region, we can detect the signal from the central pulsar if the luminosity of the pulsar exceeds 2×10^{38} erg/s in addition to the cobalt decay (for the ratio$<^{57}$Co/^{56}Co$>$ is greater than 1.7 of the solar abundance).

During the flight, the Crab Nebula was observed just before the pointing operation to SN1987A. The counting rate variation from 100keV to 200keV during this unplanned scan of the Crab Nebula is shown in Fig. 18.

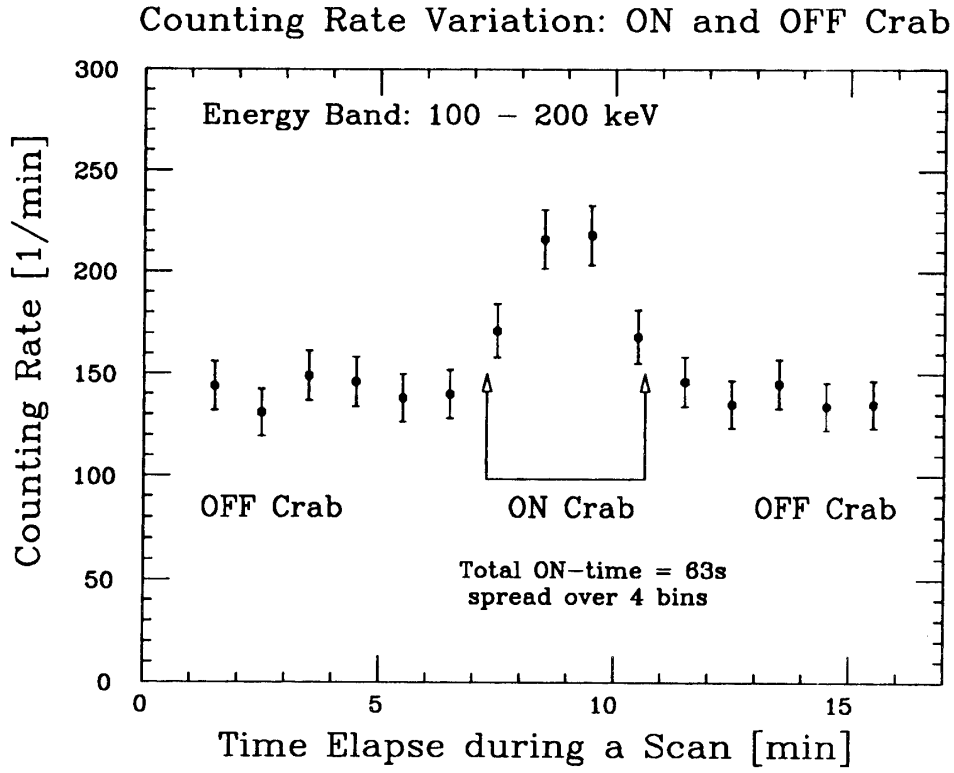

Fig. 18 Counting rate variation during the scan of the Crab Nebura for the energy range of 100−200keV: Crab Nebura was observed just before the pointing operation. According to the data from star camera, integrated observation time was about one minute.

The flux integrated over this energy range is consistent with the previous observations. Note that the signal to noise ratio reaches almost unity and this shows the excellent performance achieved by the Welcome-1 detector in hard X-ray region.

References

[1] K. Takagi and T. Fukazawa, 1983: Cerium-activated Gd_2SiO_5 single crystal scintillator, *Appl. Phys. Lett.*, **42**, 43.

[2] H. Ishibashi, K. Shimizu, and K. Susa, 1989: Cerium Doped GSO Scintillators and Its Application to Position Sensitive Detectors, *IEEE*, **NS-36**, 170.

[3] T. Takahashi *et al.*, 1990: A Pulse Shape Discriminator and an Online System for Balloon-Borne Hard X-Ray/Gamma-Ray Detector, in: *17th International Symposium on Space Technology and Science*, Tokyo.

[4] S. Kumagai *et al.*, 1991: Implications of the recent light curve of SN1987A, *Astronomy and Astro Phys.*, 5. 2.

[5] J. D. Kurfesset *al.*, 1989: *Proceedings of the GRO Science Workshop.*

要　旨

新型硬X線/ガンマ線望遠鏡 Welcome-1 及び SN 1987A の観測

高橋　忠幸・J. Braga・郡司　修一・釜江　常好・宮崎　聡
村上　浩之・A. Neri・能町　正治・関本裕太郎・田中　光明
田村　忠久・山岡　典子・山上　隆正

我々は，超新星1987Aの観測の他，超新星残骸や活動銀河核（AGN）など，信号の強度が非常に小さい宇宙起源の硬X線（60－800keV）の観測において，感度の高い測定を行うために，新しい気球搭載用観測器を開発し，1990年11月にブラジルにおいてSN1987Aからの^{57}Co及び連続成分の観測を目的とした実験を行った．実際に上空で観測されたバックグラウンドのフラックスから検出器は約40keVから850keVのエネルギー範囲に感度を持ち，10^4秒の観測を行った場合，連続スペクトルでは$2\sim3\times10^{-6}$cm^2/keV/s程度の信号を3σの確度で検出できることが示された．